DEVELOPMENT AND CHARACTERIZATION OF NANOSTRUCTURED FREQUENCY-SELECTIVE SURFACES (FSS)

Mario Marchetti*, Fabrizio Frezza**, Marco Regi*, Fabio Mazza*, Emiliano Carnà*

* University of Rome "La Sapienza", Department of Aeronautics and Astronautics Engineering
Via Eudossiana 18, 00184 Roma
Phone: +39 0644585953, Fax: +39 0644585670
e-mail: marco.regi@uniroma1.it

** University of Rome "La Sapienza", Department of Electronic Engineering
Via Eudossiana 18, 00184 Roma
Phone: + 39 0644585841, Fax: + 39 064742647
e-mail: fabrizio.frezza@uniroma1.it

ABSTRACT

The Frequency-Selective Surface (FSS) is an important application in many engineering sectors. In particular for radomes, filters and radar communications. The traditional FSS are constituted by two possible configurations: periodically-perforated metallic screens, or arrays of metallic patches printed on dielectric substrates.
Aeronautics, military and naval applications are the typical technological fields involved in the FSS developments.
The requirements of a FSS are:

- Pass-band filter behaviour
- To stealth the surface to the external observer.

With a specific design of the traditional FSS, thanks to the Floquet theorem, it is possible to select a unique frequency value of the above filter.
Solving Maxwell equations it is possible to determine the theoretical electromagnetic FSS behaviour. However, considering the complexity of the phenomena involved, only with an experimental test it is possible to perform a realistic characterization of the FSS.
With the nanotechnology, new FSS kinds are introduced. In fact, using particular matrixes (thermo-plastic and thermo-setting polymeric resins, silicones, etc.) with nanoparticles (structured and not) homogeneously dispersed, it is possible to produce a material with electromagnetic structural and mechanical requested properties. On the other hand, traditional FSSs provide only the electromagnetic properties.
For a nanostructured FSS a particular technological manufacturing process is requested, useful to obtain the following micro- and macro-properties: homogeneity, continuity and isotropic characterization (necessary to the imposed requirements).
Moreover, these innovative FSSs provide a continuous monolithic structure with a significant improvement in the reliability of the systems in which they are integrated.

1 – INTRODUCTION

Frequency-Selective Surfaces (FSSs) are periodic structures with filtering properties, traditionally manufactured either as periodically-perforated metallic screens or as arrays of metallic patches printed on dielectric substrates [1][2][30]. Applications range from the microwave region in multiband antenna systems, narrowband reflectors, radomes for active radar systems, RF absorbers, up to the far- and near-infrared portion of the spectrum as mirrors in molecular lasers, polarizers, and solar selective surfaces. However, existing FSSs suffer from three principal drawbacks. First, the conversion from requested design on a flat surface to the realistic curved surface of the typical

applications requires extensive empirical correlations. Second, because the surfaces use implanted elements comparable in size to the requested wavelength, they can exhibit unwanted passband - and grating-lobe scattering at out-of-band frequencies. Third, filtering characteristics vary with incidence angle and polarization, requiring special stabilization design. These drawbacks form the motivation for research into materials capable of exhibiting frequency-selective properties in the bulk without unwanted pass-bands or inherent limitations on their topology, for use in radomes, reflectors, or specialised space filters [3][9][10][26].

A novel approach is proposed, whereby narrowband filtering properties are created from random composite structures based on the physical resonant properties of the constituents and the geometry of micro- and nano-inclusions. In this manner, a bulk continuous material rather than a lattice formation is used to manipulate and shape the electromagnetic propagation. The novel artificial dielectrics constitute conformal FSSs to be applied by means of a uniform coating process to simple planar or complex curvilinear shapes.

The approach is guided by a theoretical design for a random mixture with frequency - selective properties, characterized by a concentric geometry for the inclusions [27]. The frequency dispersion of the proposed composite is driven by the use of a Lorentzian resonant dielectric as one of the constituent media.

The existence and availability of such resonant materials is essential for the physical realization of the proposed composite structures. This issue is discussed with an emphasis on the microwave regime, where the example of a physical resonant medium is given. Moreover, a particular theoretical model uses a lossy core for the implants, thus focusing on a lossy filtering composite medium, ideal for applications of thin absorbing films (TAF's). The use of diluted mixtures of small coated and uncoated metallic particles has been proposed in the past, but for broad-band frequency selection and with conventional nonresonant constituents. Actually, an innovative design relies on the explanation of the optical transparency of water according to the analytic theory of a dielectrics. In that model, the extreme transparency window of water (eight orders of magnitude deep) at optical frequencies was postulated to be the effect of coating the water molecule with a highly resonant shell. It is possible to use the same concentric geometry for the formulation of an artificial dielectric useful to develop an innovative nanostructured FSS. We derive the parameter dependence of the window formation that allows tailor-designing the novel structure according to prescribed specifications. Without loss of generality, it is possible to perform the analysis for spherically-shaped inclusions.

The novel complex medium is an amorphous ensemble of micro- and nano-spheres composed of a lossy core, coated with a highly resonant dielectric layer and embedded in a dielectric host (a polymeric matrix). This is an innovative application of the nanotechnologies in the electronic field [27].

In this paper the theoretical models for the design of innovative nanostructured FSSs are illustrated, and in particular the studies for the development of a dedicated software useful to evaluate the behaviour of this innovative nanomaterial.

The nanostructured FSS is constituted by a dielectric matrix (polymeric or silicone resin) with micro- and nano-particles embedded into the above matrix. For this composite nanostructured material, it is requested to have isotropy, homogeneity and continuity properties. In fact, when the nanoFSS works at high frequency, all possible material defects can significantly modify the electromagnetic behaviour of the element. This is the reason why it is necessary to define a specific sample-manufacturing procedure requested to obtain samples with the above characteristics [23][27].

Another problem is relevant to the choice of the materials. First, the matrix with a specific electromagnetic property is required. Besides, it is necessary to study different aspects as the thermal, mechanical, physical and chemical characterization of the matrix. In fact, the design of an innovative nano-FSS is not delimited only to the electromagnetic analysis, but also to the integration of it in a real operative system with specific requirements, relevant to all the operative

aspects and conditions. For example, the resistance to the flames and to the salty water are only two conditions of the all possible specific characterizations requested to certificate the nano-FSS produced. The surface of the sample must be very smooth to guarantee a well-defined control of the electromagnetic behaviour. For what concerns the mechanical properties, the static and dynamic resistance of the materials is one important parameter. Using a polymeric matrix, it is possible to ensure enough mechanical resistance both for specific electromagnetic instruments (advanced devices) and for naval/aeronautics applications (nano-FSS panel to be integrated to the boat and aircraft as an electromagnetic shield). It is possible to think also to a flexible nano-FSS useful to produce devices with very complex geometries. In this case it is necessary to choice a specific matrix (e.g. silicone materials).
A further aspect is relevant to the nanoparticles employed. The morphological characterization gives the opportunity to evaluate the possible use of a specific kind of micro- and/or nano-particles with particular properties (electromagnetic, mechanical, chemical, etc.). In this case it is possible to use simple particles (non-nanostructured) or particular elements (carbon nanotubes, for example). The manufacturing procedure for the samples preparation can be very different, with significant changes in the relevant behaviour of the nano-FSS. For example, to embed in the matrix carbon nanotubes with different alignment and purification degree, it can provide a very different behaviour of the FSS. This gives an idea of the technological problem involved in manufacturing a nano-FSS with the characteristics defined by the theoretical and numerical models. Instead, with the use of simple nanoparticles, the manufacturing procedure is much simpler.
Cost and availability of enough quantity of nanostructured materials are two fundamental parameters in the development on these innovative elements.
The nanoelements embedded in the matrix can provide other properties. For example, the carbon nanotubes are studied for the development of structural composite for aerospace applications, thermal management, electrical systems, etc. In this case it is possible to think of advanced materials with manifold properties (mechanical, thermal, chemical, and mainly electromagnetic).
As defined by the theory, the nanoparticle morphology is an important parameter. With the specific SEM analysis it is possible to perform a statistical morphological analysis of the materials employed. Nanoparticles and nanostructures (e.g. carbon nanotubes) require specific methodologies to perform reliable analysis (optical, SEM Scanning Electron Microscopy, TEM Transmission Electron Microscopy, EDX Energy Dispersive X-Ray) and characterization (particle geometry and dimensions, chemical composition, etc.).
The materials employed by the Authors to study innovative nano-FSSs are:

- matrix: polymeric and silicones
- commercial curing agent
- particles: micro powder of non-nanostructured graphite, carbon nanotubes and metal oxide.

The procedure requested for the manufacturing and testing of the samples is illustrated in the next paragraph.
It is necessary to observe that it is possible to produce two kinds of nanostructured samples: continuous and multilayer. In each case the uniformity of the sample thickness is fundamental to provide a homogeneous electromagnetic behaviour in the studied band (for example X Band).

2 – TRADITIONAL FREQUENCY-SELECTIVE SURFACE (FSS)

An array of conducting sheets periodically perforated, or of periodic metallic patches on a substrate, constitutes a frequency-selective surface (FSS) for electromagnetic waves.
The first geometry, commonly referred to as a capacitive FSS, performs similarly to a low-pass filter.

The second case, or inductive FSS, is similar to a high-pass filter (see fig 2.1). If the periodic elements within a FSS posses resonance characteristics, the inductive FSS will exhibit total transmission at wavelengths near the resonance, while the capacitive FSS will exhibit total reflection. A capacitive-type filter will consist of metallic patches deposited on a planar substrate. For the inductive-type filter, a metallic sheet (usually deposited on a substrate) is perforated with apertures.

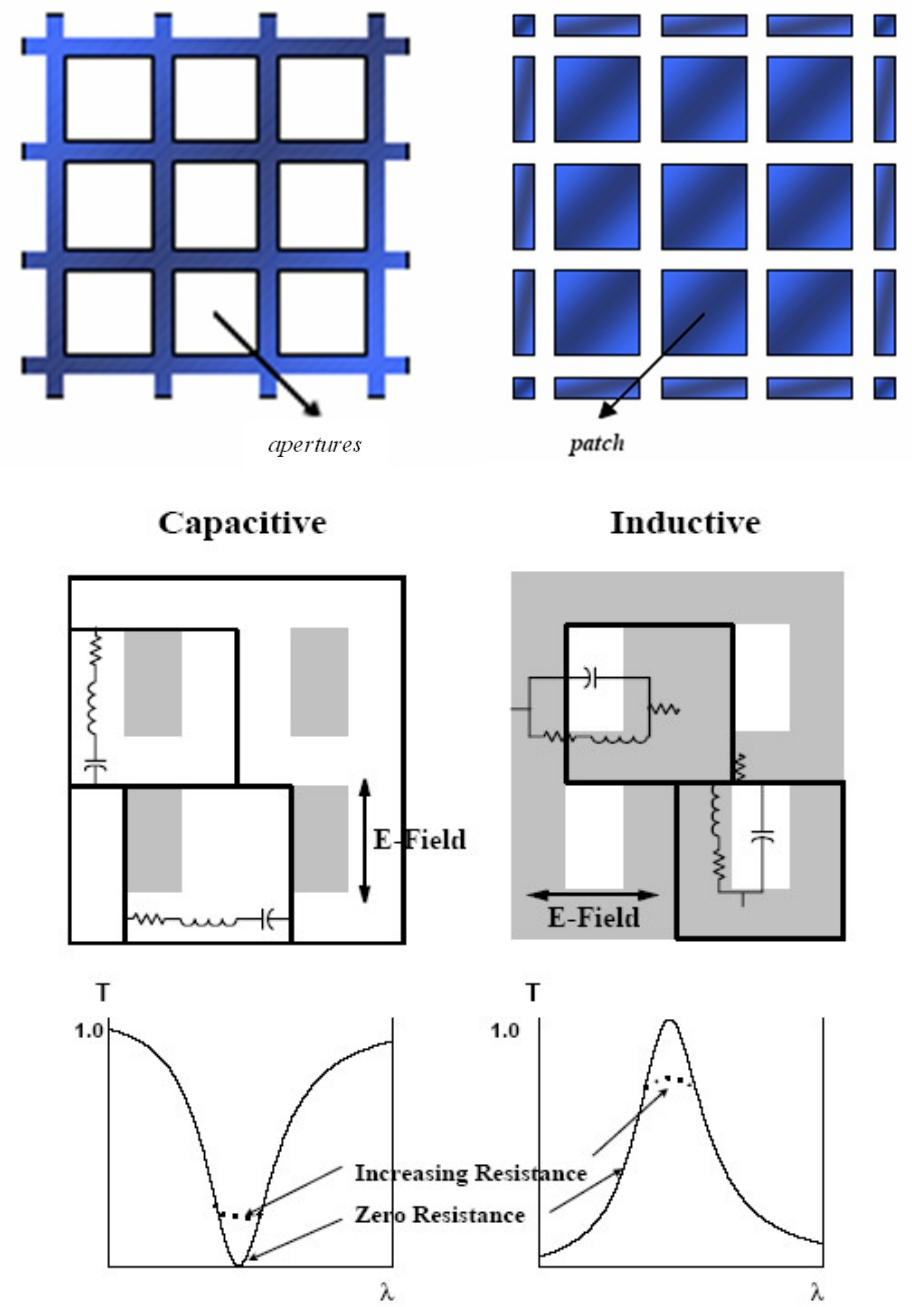

Fig. 2.1 FSS geometry, relevant capacitive and inductive behaviour (top) with corresponding equivalent circuits (middle) and their transmission profiles (bottom).

The thickness of the with respect to the wavelength at which it will be utilized determines whether the FSS is classified as “thick” or “thin”.
The periodic elements in a FSS are most commonly arranged in a rectangular array as shown in fig. 2.2. However, the more general geometric arrangement is a triangular array, also shown in fig. 2.2. Note that the periodicity in the triangular array exists along the *x*-axis, and the skewed axis.

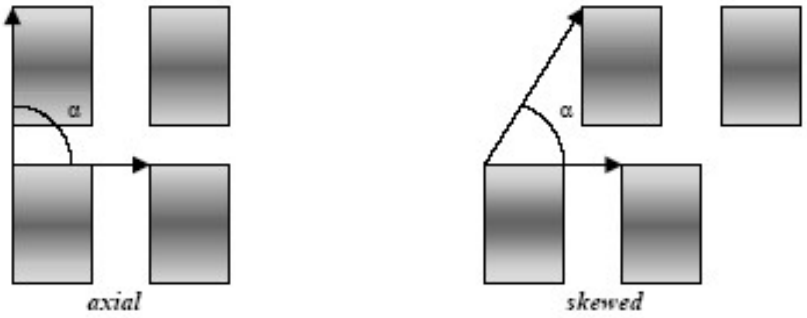

Fig. 2.2 A rectangular array and the more general triangular array of apertures (or patches) that form a FSS

Since the apertures/patches of the FSS are arranged in a periodic fashion, it is possible to describe the field at the filter plane in terms of only one unit periodic cell. *Floquet's theorem* states that if a linear differential equation has periodic coefficients and periodic boundary conditions, then the stable solutions will generally be a periodic function times an exponentially decreasing function. Through the application of this theorem, the field in any other periodic cell will be related to the reference cell in terms of an exponential function.
Now a simple analytical model is described.
The structure considered is made of a periodic array of rectangular patches on two uniaxial aisotropic dielectric layers.

$$-\frac{1}{2\omega\varepsilon}\sum_{m,n}\begin{bmatrix}\dfrac{k^2-\alpha_m^2}{\sqrt{k^2-\alpha_m^2-\beta_n^2}} & \dfrac{-\alpha_m\beta_n}{\sqrt{k^2-\alpha_m^2-\beta_n^2}}\\ \dfrac{-\alpha_m\beta_n}{\sqrt{k^2-\alpha_m^2-\beta_n^2}} & \dfrac{k^2-\beta_n^2}{\sqrt{k^2-\alpha_m^2-\beta_n^2}}\end{bmatrix}\begin{bmatrix}J_x(\alpha_m,\beta_n)\\ J_y(\alpha_m,\beta_n)\end{bmatrix}\exp\left[j(\alpha_m x+\beta_n y)\right]=-\begin{bmatrix}E_x^I(x,y)\\ E_y^I(x,y)\end{bmatrix} \tag{2.1}$$

In the above-given relation, ω denotes the angular frequency of a wave, ε is the permittivity of the surrounding of the selective surface, α_m and β_n are spatial frequencies:

$$\alpha_0 = k\sin\theta_i\cos\phi_i$$

$$\beta_0 = k\sin\theta_i\sin\phi_i$$

$$k = \frac{2\pi}{\lambda}$$

$$\alpha_m = \alpha_0 + \frac{2\pi}{a}m$$

$$\beta_n = \beta_0 + \frac{2\pi}{b}n$$

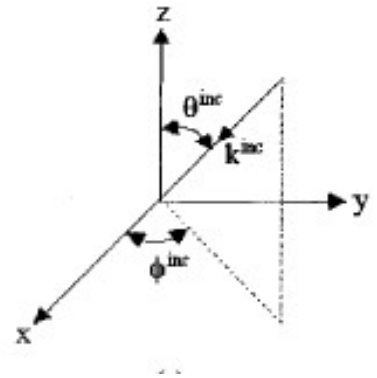

Fig.2.3 Incident plane wave

k denotes free-space wave number, J_x and J_y are components of current-density vector over the element, and finally $E_x{}^I$ and $E_y{}^I$ denote components of electric-field intensity of incident wave.
Solving the problem, we approximate the unknown current distribution in (2.1) in terms of properly-chosen basis function, and unknown approximation coefficients. Such formal approximation is substituted into equation (2.1). Since the approximation does not match the

equation exactly, we respect this fact by introducing a residual function (residuum). Smaller values the residual function reaches, more accurate the approximation is. The residuum is minimized by Galerkin Method (residuum is sequentially multiplied by as many basis functions as many unknown approximation coefficients have to be computed; in that way the set of *N* linear algebraic equations for *N* unknown approximation coefficients is obtained).
There are two approaches for choosing basis functions. The first one exploits basis functions, which are non-zero over the whole analysed area. Such functions are elected to physically represent standing waves of the current on an element.
The second approach divides the analysed region into sub-regions, where the current is approximated in terms of basis functions, whose functional value is non-zero over a given sub-region only. This approach is advantageous in simple analysis of selective surfaces consisting of arbitrarily-shaped elements.

Harmonic basis functions

Let us assume a FSS consisting of rectangular perfectly-conductive elements of dimensions *a′* and *b′*. Components of current density *J* are approximated as follows

$$\mathbf{J}(x,y) = \sum_{p=0}^{P}\sum_{q=0}^{Q} A_{pq}\Psi_{pq}^{TM} + F_{pq}\Psi_{pq}^{TE} \qquad (2.2)$$

where:

$$\Psi_{pq}^{TE}(x,y) = \left[\frac{p\pi}{a'}\sin\left(\frac{p\pi x}{a'}\right)\cos\left(\frac{q\pi y}{b'}\right)\mathbf{u}_x + \frac{q\pi}{b'}\cos\left(\frac{p\pi x}{a'}\right)\sin\left(\frac{q\pi y}{b'}\right)\mathbf{u}_y\right]\exp\left[j(\alpha_0 x + \beta_0 y)\right]$$
$$\Psi_{pq}^{TM}(x,y) = \left[\frac{p\pi}{b'}\sin\left(\frac{p\pi x}{a'}\right)\cos\left(\frac{q\pi y}{b'}\right)\mathbf{u}_x - \frac{q\pi}{a'}\cos\left(\frac{p\pi x}{a'}\right)\sin\left(\frac{q\pi y}{b'}\right)\mathbf{u}_y\right]\exp\left[j(\alpha_0 x + \beta_0 y)\right] \qquad (2.3)$$

Here, Ψ_{pq}^{TE} and Ψ_{pq}^{TM} are two different functions for parallel polarization and perpendicular one. These functions differ in two aspects:

- indices *p*, *q* for the function Y_{pq}^{TE} can reach zero, while for Y_{pq}^{TM} are one or higher
- component J_y for perpendicular polarization has to be of the opposite sign to J_y for parallel polarization.

Combination of harmonic functions and Chebyshev polynomials

$$\mathbf{J}^{TE} = \sin\left[\frac{p\pi}{a'}\left(x+\frac{a'}{2}\right)\right]\frac{T_q(2y/b')}{\sqrt{1-(2y/b')^2}}\mathbf{x} + \frac{T_p(2x/a')}{\sqrt{1-(2x/a')^2}}\sin\left[\frac{q\pi}{b'}\left(y+\frac{b'}{2}\right)\right]\mathbf{y}$$
$$\mathbf{J}^{TM} = \sin\left[\frac{p\pi}{a'}\left(x+\frac{a'}{2}\right)\right]\frac{T_q(2y/b')}{\sqrt{1-(2y/b')^2}}\mathbf{x} - \frac{T_p(2x/a')}{\sqrt{1-(2x/a')^2}}\sin\left[\frac{q\pi}{b'}\left(y+\frac{b'}{2}\right)\right]\mathbf{y} \qquad (2.4)$$

In contrast to harmonic basis functions, the function cosine is replaced by *Chebyshev polynomial* in order to reach infinite values at the edges of elements. That way, currents flowing along edges are correctly modelled.
Now, eqn. (2.1) is solved by Galerkin method: eqn. (2.1) is sequentially multiplied by basis functions and the product is integrated over the surface of the element. For purely harmonic basis functions, we get:

$$\int_a^b w_m(z)\,R(z)\,dz = 0 \qquad m = 0, 1, \ldots N$$

$$\sum_{p,q} A_{pq} \left\{ \sum_{m,n} \Psi_{rs}^{TM*}(\alpha_m, \beta_n)\, K(\alpha_m, \beta_n)\, \Psi_{pq}^{TE*}(\alpha_m, \beta_n) \right\} + \tag{2.5}$$

$$+ F_{pq} \left\{ \sum_{m,n} \Psi_{rs}^{TE*}(\alpha_m, \beta_n)\, K(\alpha_m, \beta_n)\, \Psi_{pq}^{TE*}(\alpha_m, \beta_n) \right\} = \frac{-1}{ab} \iint_{\substack{pres \\ element}} E_{\tan}^{I}(x,y)\, \Psi_{rs}^{TE*}(x,y)\, dx\, dy$$

$$\sum_{p,q} A_{pq} \left\{ \sum_{m,n} \Psi_{rs}^{TM*}(\alpha_m, \beta_n)\, K(\alpha_m, \beta_n)\, \Psi_{pq}^{TM*}(\alpha_m, \beta_n) \right\} + \tag{2.6}$$

$$+ F_{pq} \left\{ \sum_{m,n} \Psi_{rs}^{TM*}(\alpha_m, \beta_n)\, K(\alpha_m, \beta_n)\, \Psi_{pq}^{TE*}(\alpha_m, \beta_n) \right\} = \frac{-1}{ab} \iint_{\substack{pres \\ element}} E_{\tan}^{I}(x,y)\, \Psi_{rs}^{TM*}(x,y)\, dx\, dy$$

If the above-given set is solved out, electric intensity $\boldsymbol{E}^{S}$ in spectral domain is computed. Intensity $\boldsymbol{E}^{S}$ appears at the left-hand side of eqn. (2.1)

$$\mathbf{E}^{S} = -\frac{1}{2\omega\varepsilon} \sum_{m,n} \begin{bmatrix} \dfrac{k^2 - \alpha_m^2}{\sqrt{k^2 - \alpha_m^2 - \beta_n^2}} & \dfrac{-\alpha_m \beta_n}{\sqrt{k^2 - \alpha_m^2 - \beta_n^2}} \\ \dfrac{-\alpha_m \beta_n}{\sqrt{k^2 - \alpha_m^2 - \beta_n^2}} & \dfrac{k^2 - \beta_n^2}{\sqrt{k^2 - \alpha_m^2 - \beta_n^2}} \end{bmatrix} \begin{bmatrix} J_x(\alpha_m, \beta_n) \\ J_y(\alpha_m, \beta_n) \end{bmatrix} e^{j(\alpha_m x + \beta_n y)} = -\begin{bmatrix} E_x^I(x,y) \\ E_y^I(x,y) \end{bmatrix}$$

Computing electric intensity of scattered wave $\boldsymbol{E}^{S} = \mathbf{E}^{R}$, only the basic harmonic component on the frequency a_0, b_0 is assumed. If the period a is small (smaller than one half of the wavelength) and frequency approaches the first resonance of the surface, then a uniform field of the scattered wave exists in the far field region only. If the condition is not satisfied, then parasitic modes can be excited (higher spatial frequencies are not filtered by the near-field zone, and corresponding waves propagate further).

3 – NANOSTRUCTURED POLYMERIC FREQUENCY-SELECTIVE SURFACE (FSS)

In this paragraph the manufacturing process of the nanostructured composite materials, and the relevant characterizations, are illustrated.
The specific procedure employed is summarised as follows:

- choice of the appropriate materials (matrix, curing agent, micro- and nano-particles and nanostructured materials)
- to study the sample production methodologies (out gassing of the polymer in vacuum chamber; curing thermal conditions; quantities of the nanomaterial, evaluated in % wt, to be embedded in the matrix; mould preparation; etc.)
- to obtain a uniform distribution of the micro- and nano-particles (graphite, carbon nanotubes, metal oxide) in the matrix (polymeric, silicone, etc.)
- numerical prediction of the sample behaviour

- to perform morphological and mechanical tests (dynamic and static) of the sample
- to perform electromagnetic tests for the behaviour evaluation of the nano-FSSs developed (evaluation of the scattering matrix and of the electrical permittivity ε and magnetic permeability μ)
- comparisons between the experimental and theoretical results
- improvement of the nanocomposite characteristics as function of the information provided by the above test
- to determine possible applications of the nano-FSSs tested, as a function of the results obtained and of the requirements imposed by advanced electromagnetic systems for naval and aerospace applications.

The preliminary activities are devoted to the sample manufacturing (Fig. 3.1), useful to obtain materials with specific parameters (dimensions, geometry, porosity, roughness, etc.). The base materials employed are: epoxy resin, commercial curing agents, nanoparticles of graphite (mean dimensions: < 20 μm).

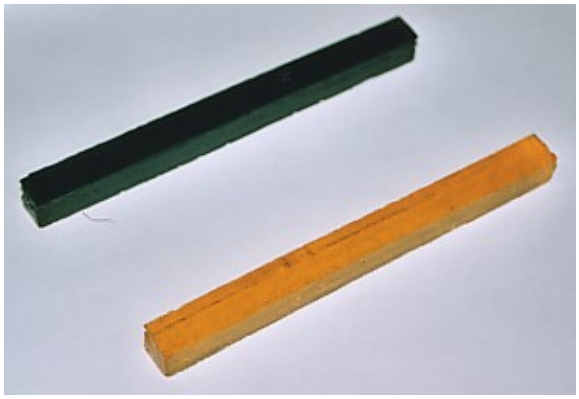

Fig. 3.1 preliminary sample manufacturing [21]

With these sample it is possible to perform a static and dynamic mechanical test (fig. 3.2), that provides important results on the structural behaviour of this material that will be employed for electromagnetic applications.

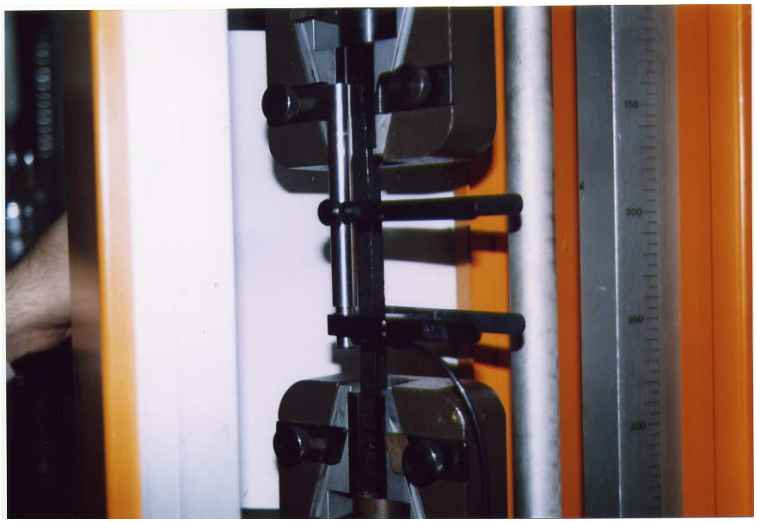

Fig. 3.2 mechanical test of the nanostructured composite samples

Using the SEM, a fracture-section characterization is also possible (fig. 3.2). This allows us to investigate the internal morphology of the materials and the micromechanics composite behaviour.

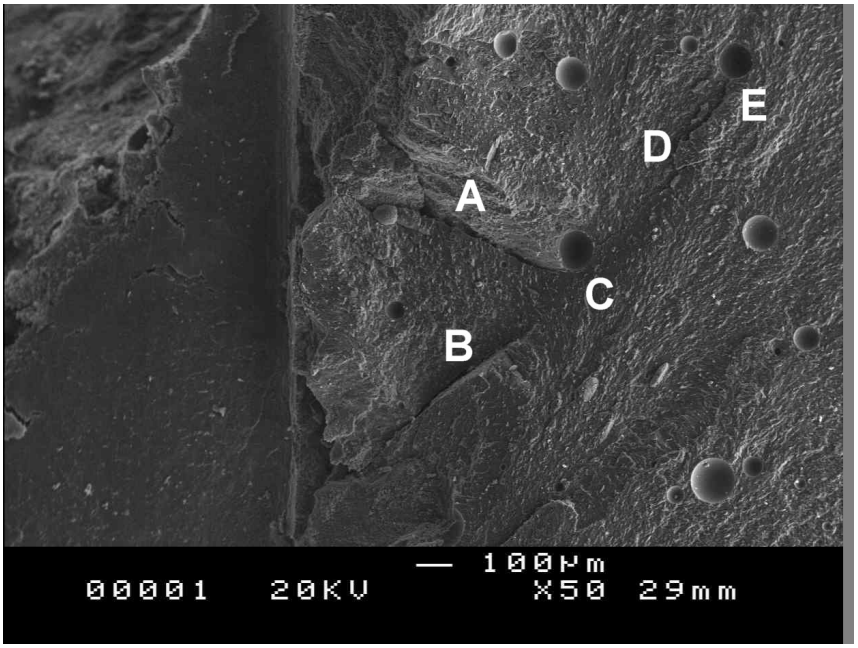

Fig. 3.3 SEM analysis of the sample (ref. Fig. 3.1), micro–cracks are indicated by white letters [21]

The experimental results indicate that, with the carbon microparticles embedded on the polymeric matrix the Young Modulus improvement is more than 12%. This is an important result, because shows how this materials offers, besides the electromagnetic properties, specific mechanical characteristics.
To perform a NDT (No Destructive Testing) ultrasonic test a massive plate is requested. To avoids the vacuum inclusions in the materials, a VARTM (Vacuum Resins Transfer Moulding) is developed (Fig. 3.4 – 3.5), using the same base materials employed in the previous samples manufacture.


Fig. 3.4 VARTM methods developed for the manufacturing of the nanostructured polymeric composite plate

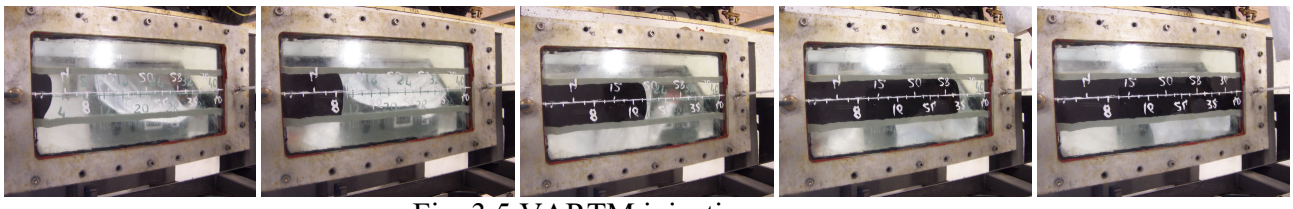
Fig. 3.5 VARTM injection sequence

The VARTM technique provides samples with very high smooth surface and without inclusion in the internal regions of the material. NDT ultrasonic test spectra (fig. 3.6) show that the sample has the requested properties, i.e., homogeneity, continuity and isotropic characteristics, evaluated in the micro-scale dimensions.

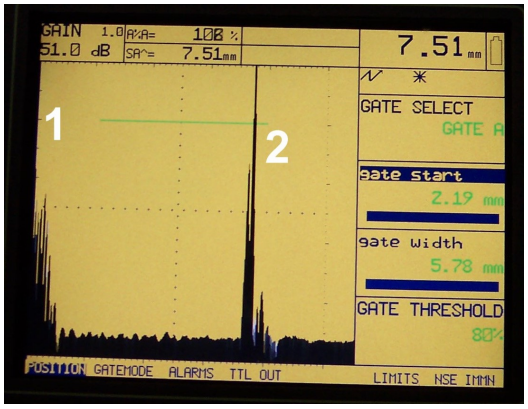

Fig. 3.6 NDT ultrasonic test on the sample showed in fig. 3.4

Another important test is the SEM characterization of the particles embedded in the matrix. Using a specific sample preparation procedure (developed by the Authors) the micro- and nano-particles have been observed by the SEM (fig. 3.7).

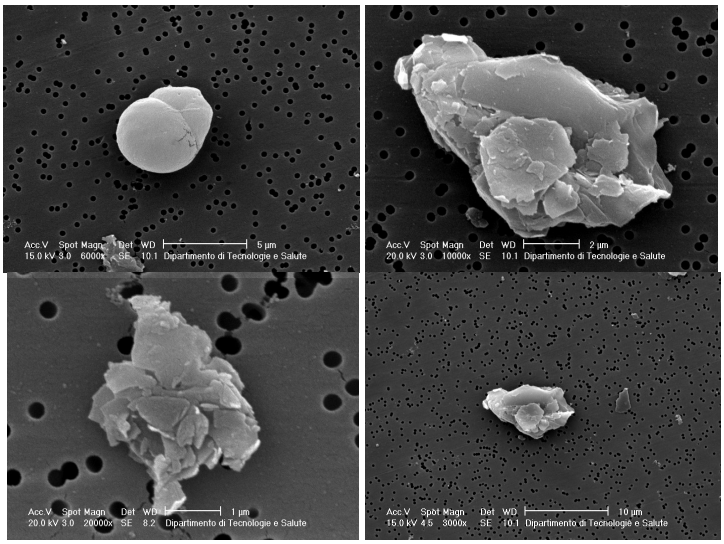

Fig. 3.7 SEM observation of the micro- and nano-carbon particles employed in the nanostructured polymeric composite materials

With a specific software integrated in the SEM, a statistic analysis of the particle dimension is performed. It is necessary to individuate a region in which numerous micro- and/or nano-particles are present, and then to define the range dimensions to study. In this case, the software determines a particles groups, each with a specific range dimension (indicated by different colours in the SEM micrograph reported in Fig. 3.8).

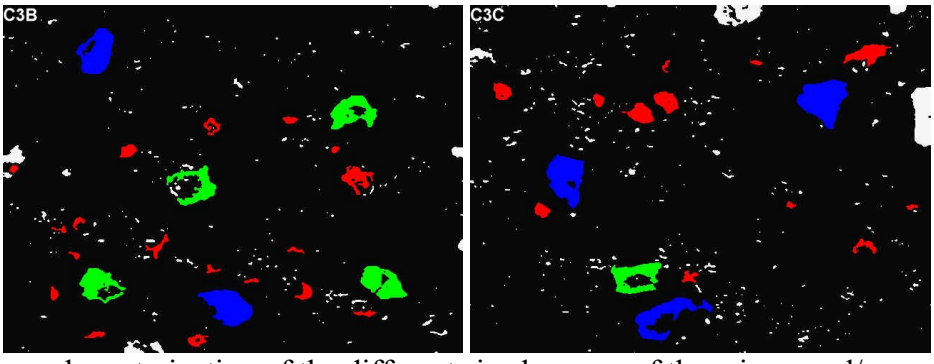

Fig. 3.8 colour characterization of the different sized groups of the micro- and/or nano-particles observed by SEM (Sample n° 1 and n° 2)

	ID Particle	ID Class	Area	Diameter Mean	Diameter Max	Diameter Min	Perimeter
			µm²	µm	µm	µm	µm
SAMPLE n° 1 (fig. 3.8 left)							
	1	3	8,11	3,77	4,25	3,08	15,98
	2	2	6,73	3,83	4,19	3,12	17,71
	3	1	0,60	1,14	1,38	0,65	3,17
	4	1	1,00	1,47	1,53	1,32	7,97
	5	1	1,20	1,42	1,57	1,10	4,25
	6	1	0,32	0,68	0,74	0,61	2,05
	7	1	0,35	0,71	0,78	0,67	2,19
	8	2	5,48	4,08	4,45	3,15	21,60
	9	1	3,22	2,66	2,88	2,36	14,44
	10	1	0,53	1,08	1,16	0,84	3,84
	11	1	0,33	1,15	1,37	0,62	3,47
	12	1	1,07	2,12	2,34	1,53	7,38
	13	1	0,39	1,33	1,57	0,58	3,67
	14	1	0,33	0,92	1,08	0,57	2,68
	15	1	0,42	1,12	1,26	0,75	3,61
	16	2	6,98	3,75	4,42	2,48	16,15
	17	2	6,01	3,58	4,08	2,83	19,00
	18	1	0,33	1,13	1,30	0,53	2,91
	19	1	1,13	1,52	1,59	1,46	5,10
	20	1	0,59	1,09	1,26	0,71	3,13
	21	3	9,10	4,26	5,08	2,99	13,66
	22	1	0,62	1,75	2,05	0,62	4,62
	23	1	0,64	1,59	1,81	0,61	4,09
	24	1	1,10	1,55	1,80	1,12	6,38
mean			**2,36**	**1,99**	**2,25**	**1,43**	**7,88**
max			**9,10**	**4,26**	**5,08**	**3,15**	**21,60**
min			**0,32**	**0,68**	**0,74**	**0,53**	**2,05**
SAMPLE n° 2 (fig. 3.8 right)							
	1	1	3,75	3,61	4,35	1,91	10,87
	2	1	0,32	0,99	1,10	0,75	3,29
	3	1	0,32	0,94	1,14	0,42	2,50
	4	3	11,33	4,42	4,55	4,14	14,48
	5	1	1,73	1,66	1,89	1,39	5,91
	6	1	2,64	2,09	2,47	1,60	6,89
	7	1	0,80	1,09	1,26	0,86	3,41
	8	1	2,75	2,42	2,92	1,67	7,49
	9	3	9,56	4,22	4,90	3,25	15,74
	10	1	0,31	0,76	0,88	0,53	2,31
	11	1	1,18	1,35	1,47	1,03	4,19
	12	1	0,31	0,89	1,06	0,50	2,48
	13	1	1,12	1,86	2,11	1,44	7,25
	14	2	6,54	4,25	4,51	2,94	20,41
	15	1	0,85	1,41	1,59	1,16	5,27
	16	3	8,41	5,97	6,86	3,04	24,61
mean			**3,24**	**2,37**	**2,69**	**1,66**	**8,57**
max			**11,33**	**5,97**	**6,86**	**4,14**	**24,61**
min			**0,31**	**0,76**	**0,88**	**0,42**	**2,31**

Tab. 1 SEM statistical analysis of the carbon particles used in the nanostructured polymeric composite materials

Tab. 1 provides the numerical results of the statistical particle dimensions analysis performed by the software integrated in the SEM.
It is interesting to produce thin films with the same materials used in the previous activities. With the same procedures four film are released (fig. 3.9). Tab. 2 illustrates the thickness measurement.

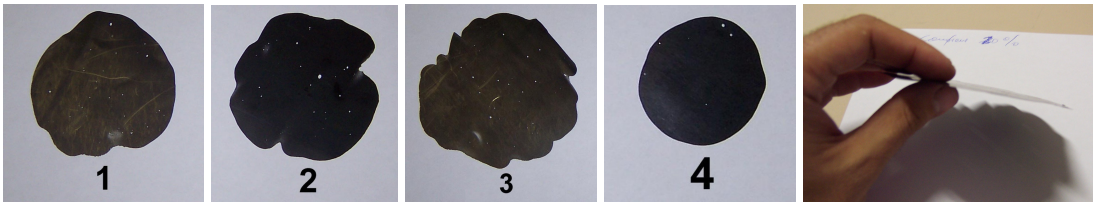

Fig. 3.9 thin films

Thin film n°/ Thickness [µm]	measure n° 1	measure n° 2	measure n° 3	measure n° 4	measure n° 5
1	280	240	270	280	270
2	240	300	220	270	270
3	320	290	485	290	350
4	300	240	270	260	210

Tab. 2 thin films thickness measurement

The use of polymeric nanostructured thin films is another important possible application for structural innovative nano–FSS.
After these material characterizations it is possible to produce nanostructured FSS samples. The electromagnetic test will be performed in the X band (see paragraph 4).
The materials employed are:

1. graphite (0%, 50%, 65% in wt respect the resin + curing agent)
2. epoxy and polyester resin and silicone
3. curing agent.

For each material a specific curing cycle has been adopted, as specified by the materials datasheet and by the curing test performed by the Authors. It is important to note that the curing process of the matrixes can vary in significant way when the particles are embedded on it.
Figures 3.10÷3.12 show the various methodologies and phases of the sample manufacturing.

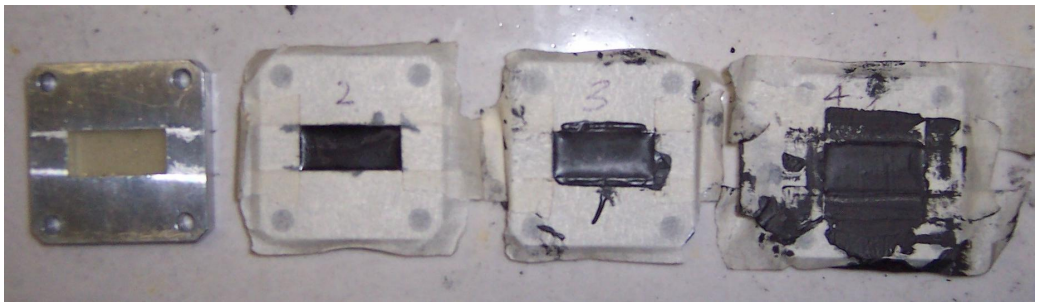

Fig. 3.10 nanostructured samples FSS manufacture procedures


Fig. 3.11 nanostructured samples FSS manufacture procedures

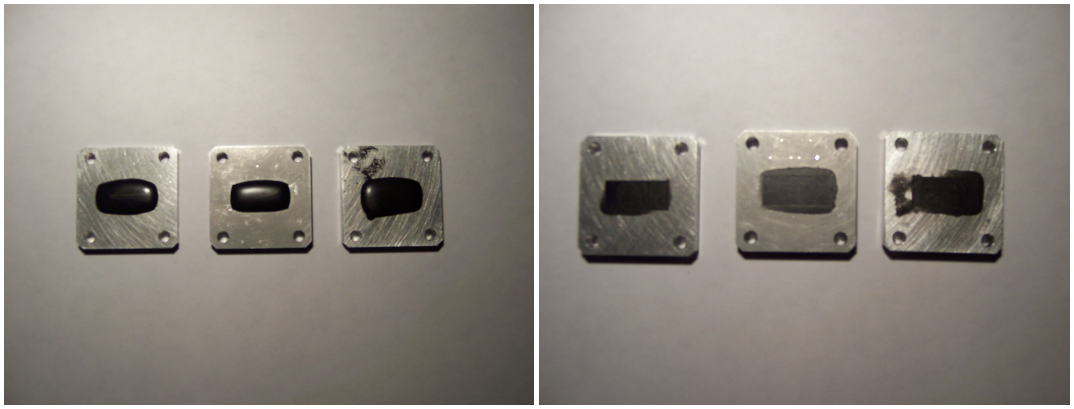

Fig. 3.11 nanostructured FSS samples (before the final mechanical removal of the residual material on the wave-guide surfaces)

At the INFN of Frascati (Nanotechnology Laboratory, Director Dr. Stefano Bellucci) a Thermal CVD facility (fig. 3.12) has been developed, useful to the synthesis of carbon nanotubes (with the typical thermal synthesis temperature profile reported in Fig. 3.13). This nanomaterial, in the literature [11÷20], is indicated as a possible innovative "element" in the development of structural FSSs.
Fig. 3.14 shows SEM micrographs of carbon nanotubes bundles growth in a *Si* – 100 (drugged and nickel coated) substrate. Fig. 3.15 indicates that the structures observed by SEM, effectively, are carbon nanotubes (bamboo like multiwall carbon nanotubes). Figures 3.16&17 illustrate the AFM analysis performed on the carbon nanotubes synthesized [22], and fig. 3.18 the EDX chemical analysis.

Fig. 3.12 Thermal CVD facility developed [23]

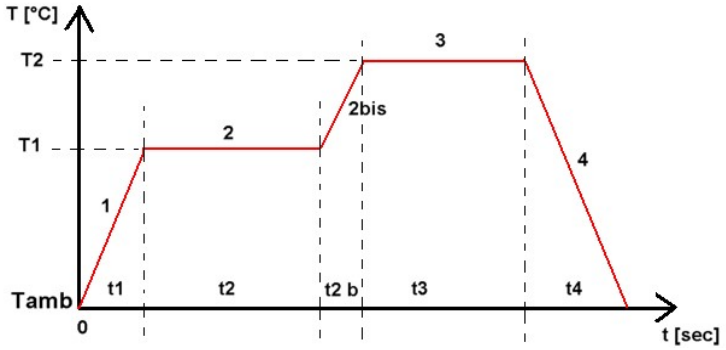

Fig. 3.13 Thermal CVD synthesis temperature (*T*) profile

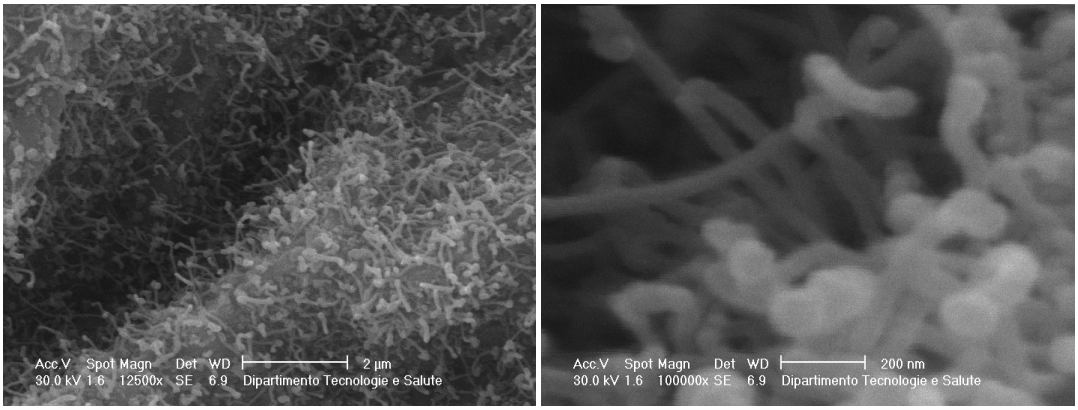

Fig. 3.14 SEM pictures of the carbon nanotubes bundles synthesized by Thermal CVD (*free - standing* growth direction) [23]

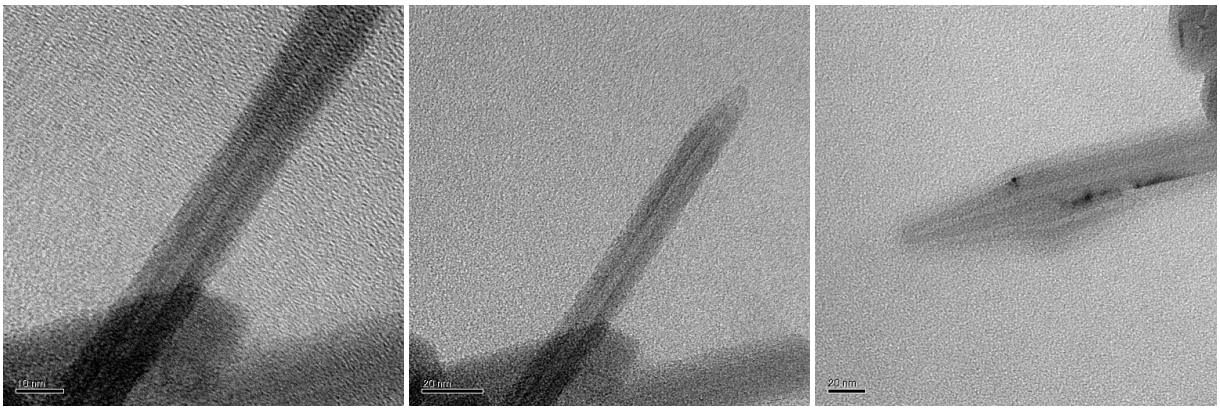

Fig. 3.15 carbon nanotubes HRTEM micrographs [23]

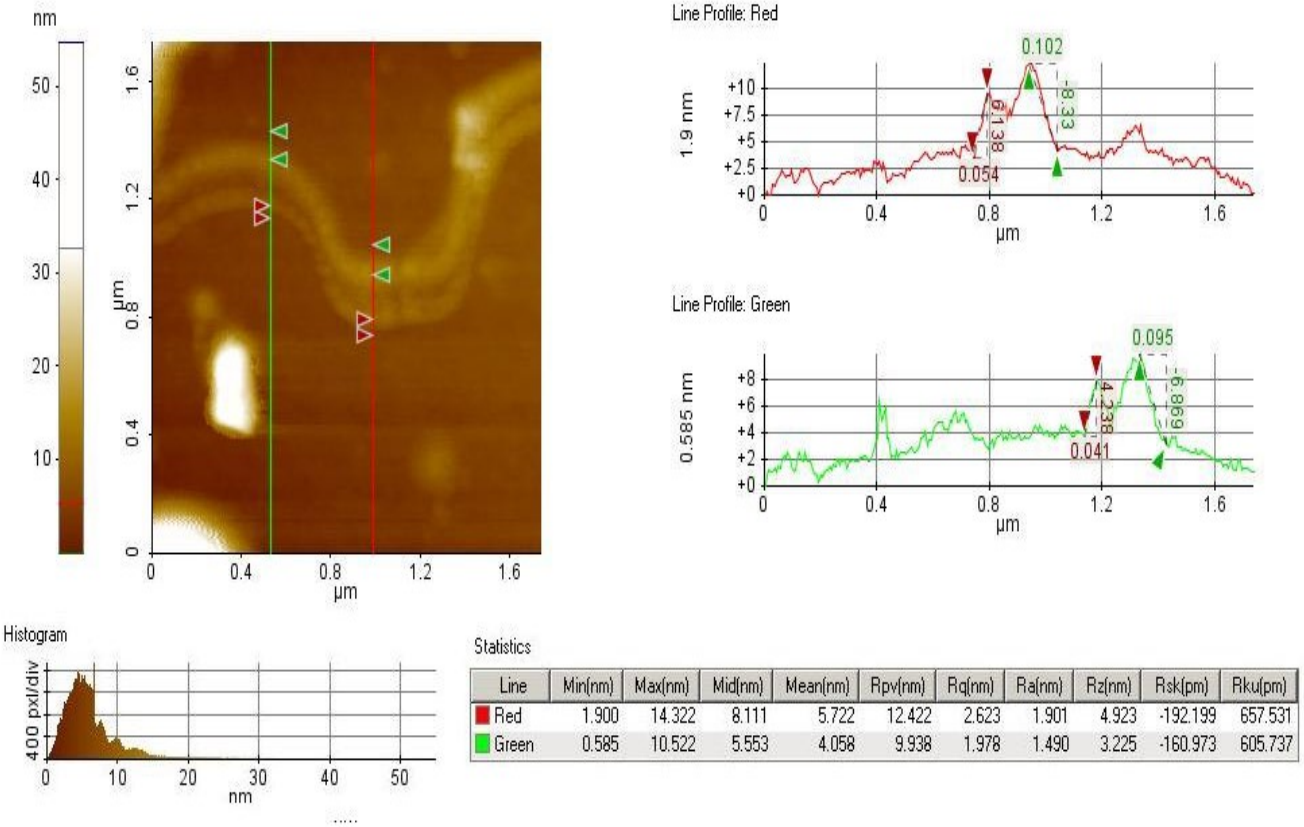

Line	Min(nm)	Max(nm)	Mid(nm)	Mean(nm)	Rpv(nm)	Rq(nm)	Ra(nm)	Rz(nm)	Rsk(pm)	Rku(pm)
Red	1.900	14.322	8.111	5.722	12.422	2.623	1.901	4.923	-192.199	657.531
Green	0.585	10.522	5.553	4.058	9.938	1.978	1.490	3.225	-160.973	605.737

Fig. 3.16 AFM analysis of the carbon nanotubes [22]

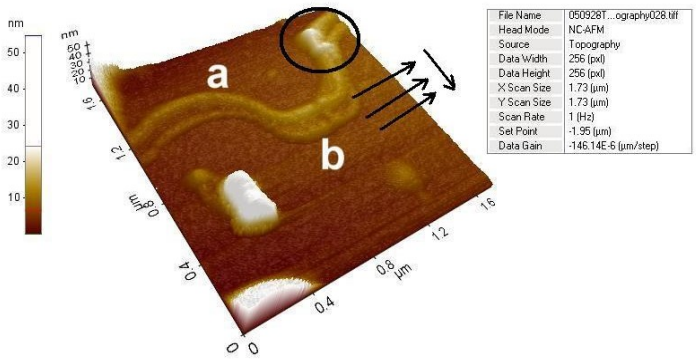

Fig. 3.17 AFM analysis of the carbon nanotubes [22]

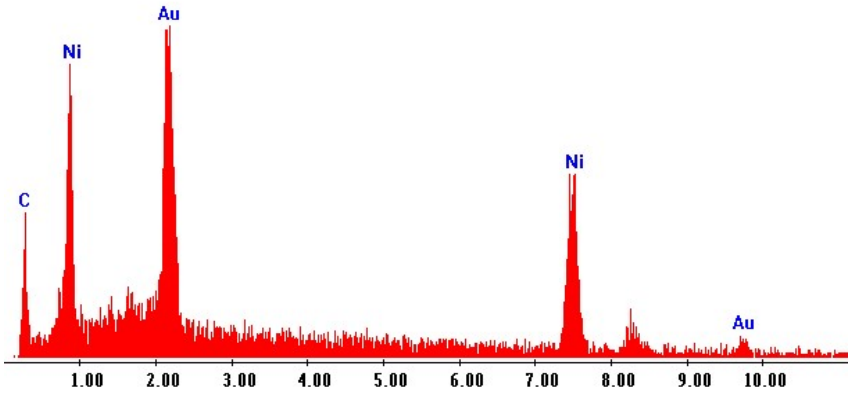

Fig. 3.18 EDX analysis of the carbon nanotubes produced

In this paragraph have been illustrated the activities relevant to the innovative nanostructured polymeric composite materials useful to the design of innovative nanostructured Frequency-Selective Surfaces (FSS). The experimental tests, performed to evaluate the electromagnetic behaviour are discussed in the next paragraph.

4 – EXPERIMENTAL TEST

To experimentally characterize the fabricated materials, even if we had at disposal an anechoic-chamber setup, we chose to begin to work in a more controllable waveguide (closed) environment, in such a way avoiding problems related to a free-space measurement, particularly with reference to the finite size of the fabricated samples (edge effects).
To this aim, we prepare samples of the same size as a rectangular waveguide (WR90) in the X frequency band, that is from 8.20 to 12.40 GHz.
Moreover, we employed a vector network analyzer Agilent Portable Network Analyzer (PNA) E8363B (fig. 4.1), which is able to measure the scattering *S* parameters (in magnitude and phase) of any microwave two-port device under test (DUT) connected to the instrument, from 10 MHz to 40 GHz.
Since the input and output interfaces of the PNA are realized with precision 2.4 mm coaxial cables (to make measurements possible up to 40 GHz), we employed suitable adaptors from 2.4 mm connectors to 3.5 mm coaxial cables (usually employed for measurements up to 26.5 GHz), then transitions from 3.5 mm coaxial connectors to WR-90 rectangular waveguide (precision Maury Microwave components).
Finally, it was necessary to perform an accurate calibration of the instrument, in such a way to eliminate the effects of the various transitions on the performances of the DUT. Employing two straight stubs in WR-90 rectangular waveguide to cope with the presence of higher-order modes excited at the coax-waveguide transitions.

In Fig. 4.3, as a preliminary example, is reported in *dB* the frequency response from 8 to 12 GHz of the bulk resin material. The magnitude of the scattering parameter S_{21} (that is, the response at port 2 when port 1 is excited), defined as:

$$S_{21}(dB) = 10\lg_{10}\frac{P_{out}}{P_{in}} \qquad (4.1)$$

where:

P_{out} = electromagnetic power measured at port 2
P_{in} = electromagnetic power measured at port 1.

In particular, P_{in} indicates the power acting on the nanostructured materials (deposited in the waveguide, see fig. 3.10), and P_{out} the transmitted power through the nanomaterials itself.
In easy way:

if $P_{out} = P_{in} \rightarrow dB = 0$
if $P_{out} < P_{in} \rightarrow dB < 0$ (in this case the material absorbs the electromagnetic power acting on it).

As described in Paragraph 1, in the study of FSSs, other two important physical parameters are:

electrical permittivity (ε):
provides the electrical behaviour of the material = Re(ε) + j Im(ε) $\Rightarrow \varepsilon_c = \varepsilon$ - j (σ/ω), with σ = loss power due to Joule effect, $\omega = 2\pi f$ (f = frequency)
with Re(ε) always > 0 (capacitive effect = electric energy absorption)
by Poynting Theorem: Im(ε) > 0 (active material); Im(ε) < 0 (electrical power loss).

magnetic permeability (μ):
provide the magnetic behaviour of the material = Re(μ) + j Im(μ)
with Re(μ) always > 0 (inductive effect = magnetic energy absorption)
by Poynting Theorem: Im(μ) > 0 (active material); Im(μ) < 0 (magnetic power loss).

In the case of FSSs, it is necessary to obtain the following general results: [Im(ε), Im(μ)] < 0 (the specific values will depend on the materials employed)
In the case of a "*Metamaterial*" it may be: [Re(ε), Re(μ)] < 0.

Fig. 4.1 Agilent Portable Network Analyzer (PNA) E8363B – experimental set up

The experimental electromagnetic tests are performed on the following samples (fig. 4.2, before the mechanical rework useful to obtain a smooth external surface):

1. dielectric host (polyester resin + curing agent)
2. polyester resins + curing agent + graphite micropowders (Aldrich, < 20 μm, see statistical SEM analysis showed in tab. 1, 50 and 65 % in wt with respect resin + curing agent weight)
3. silicone host.

For each typology five samples have been produced and tested.

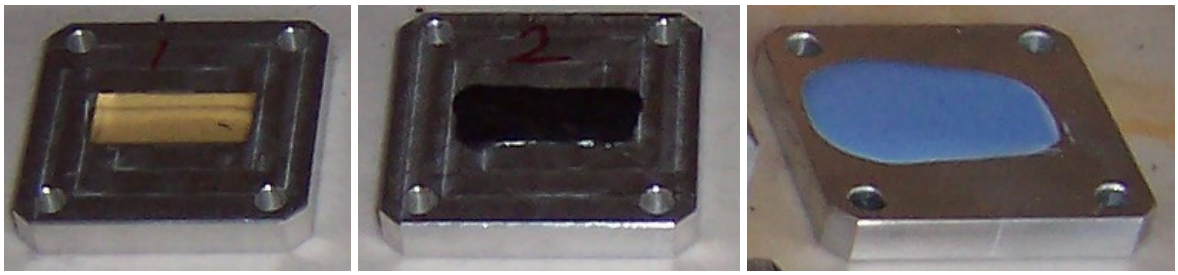

Fig. 4.2 samples: dielectric host (left), with graphite (centre) and silicone (right)

With PNA facility (fig. 4.1) the S_{21} measurements, of the above samples have been performed.
Figs. 4.3 and 4.4 illustrate the electromagnetic behaviour of the dielectric host sample (n° 1). These represent the reference data. In fact, the results provided by the sample n° 2 (host + graphite micropowders) will analysed with respect to the host.
Sample n° 1 provided the following data (fig. 4.3):

- mean electromagnetic power loss ~ 2.5÷3 dB
- minimum electromagnetic power loss ~ 0.5 dB
- max electromagnetic power loss ~ 5 dB.

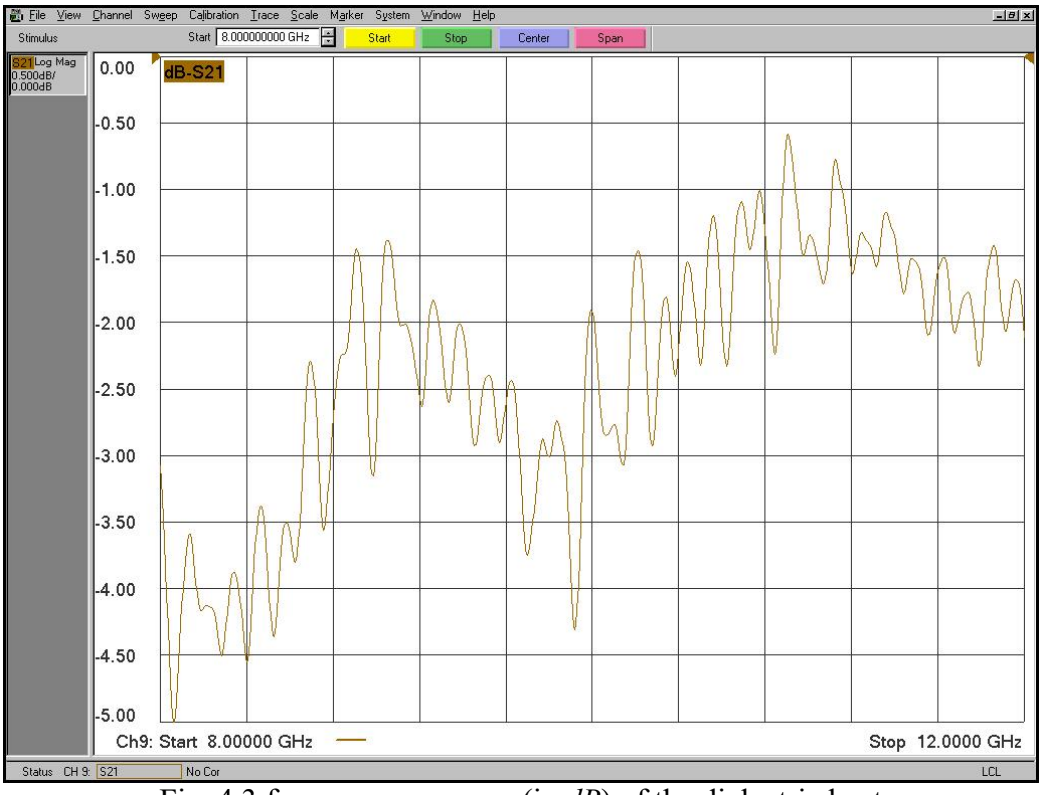

Fig. 4.3 frequency response (in *dB*) of the dielectric host

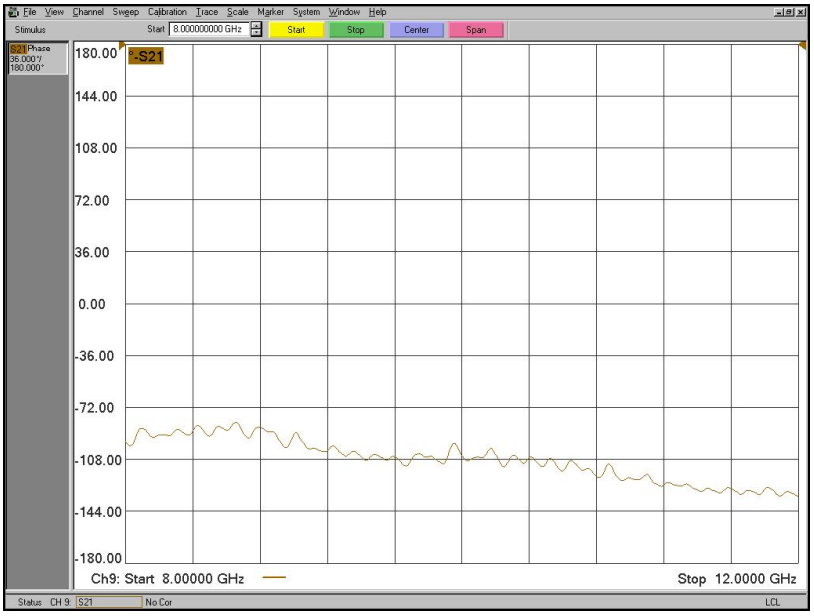

Fig. 4.4 frequency response (phase *in degrees*) of the dielectric host

Instead, sample n° 2 (dielectric host + 50% in wt of powder graphite) showed a different electromagnetic behaviour (fig. 4.5):

- mean electromagnetic power loss ~ 25÷27 dB.

With these results, it is possible to observe that:

- the electromagnetic power absorbed by materials (dielectric + graphite) is increased with respect to the host. This indicates that the micro- and nano-inclusions embedded on the polymeric matrix allow to reduce the transmitted power
- the curve presents minor oscillations (fig. 4.5) with respect to the host case (fig. 4.3). This indicates a good level of homogeneity, continuity and isotropy of the materials produced, validating, also, the manufacturing procedures developed.

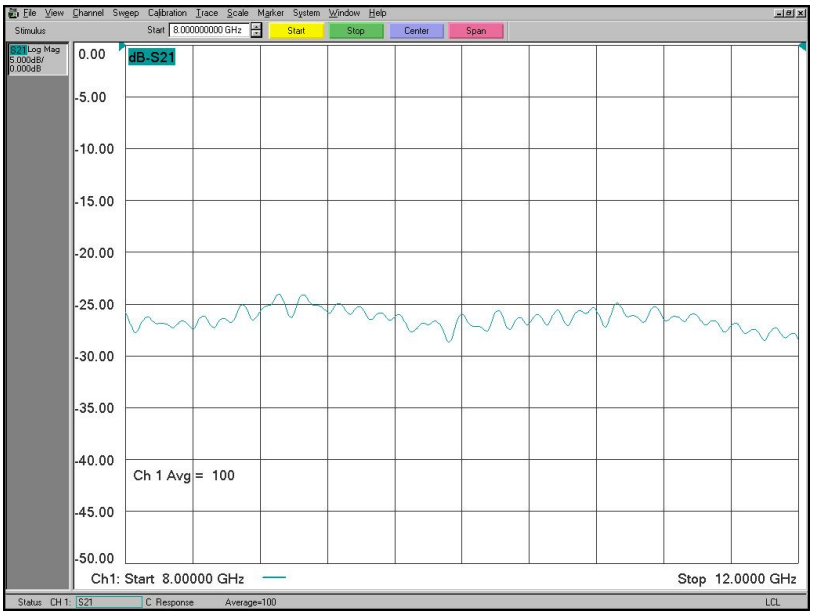

Fig. 4.5 frequency response (magnitude in *dB*) of the sample with 50% in wt of graphite

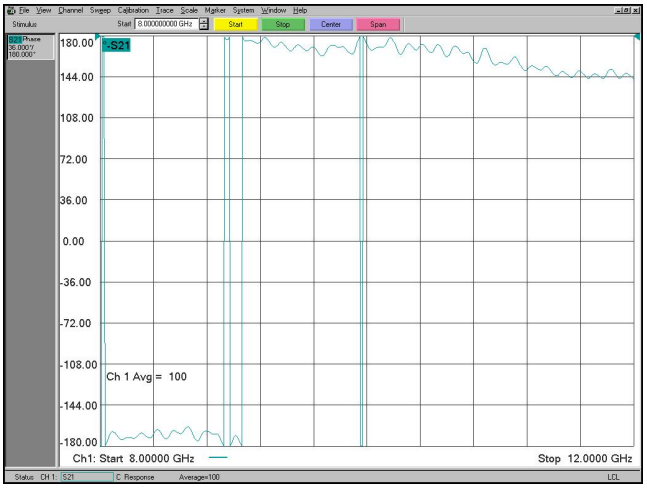

Fig. 4.6 frequency response (phase *in degrees*) of the sample with 50% in wt of graphite

Figures 4.7 and 4.8 show important results. In fact, increasing the quantity of the carbon particles embedded in the polymeric matrix, the electromagnetic power absorption increases (mean value ~ 32.5 *dB*) and the P_{out} decrease (respect a same value of P_{in}). It is possible to observe analogous results measuring the electrical permittivity (ε) and the magnetic permeability (μ). In fact, if the percentage of the micro- and nano- carbon particles, embedded in the polymeric matrix, increases, the following results are obtained:

$$\left|\mathrm{Im}(\varepsilon)\right| \uparrow \; with \; \mathrm{Im}(\varepsilon) < 0 \quad \text{and} \quad \left|\mathrm{Re}(\varepsilon)\right| \uparrow \; with \; \mathrm{Re}(\varepsilon) > 0$$
$$\left|\mathrm{Im}(\mu)\right| \uparrow \; with \; \mathrm{Im}(\mu) < 0 \quad \text{and} \quad \left|\mathrm{Re}(\mu)\right| \uparrow \; with \; \mathrm{Re}(\mu) > 0$$

Besides, fig. 4.9 and 4.10 illustrate the data relevant to the silicone sample (n° 3). The electromagnetic behaviour is very similar with respect to the dielectric host. The inclusion on the micro- and nano-particles is the silicone host in under evaluation. The use of the silicone materials is indicated due to the possibility to produced flexible FSSs, with the important possibility to produce FSS elements with a complex shape.
Then, the principal characterization of these innovative materials are:

- a specific electromagnetic behaviour
- to provide mechanical and thermal properties
- to select a definite frequency in which S_{21} ~ 100% and S_{12} ~ 0% (expressed in terms of the percentage of the external power excitation acting on the FSS surface).

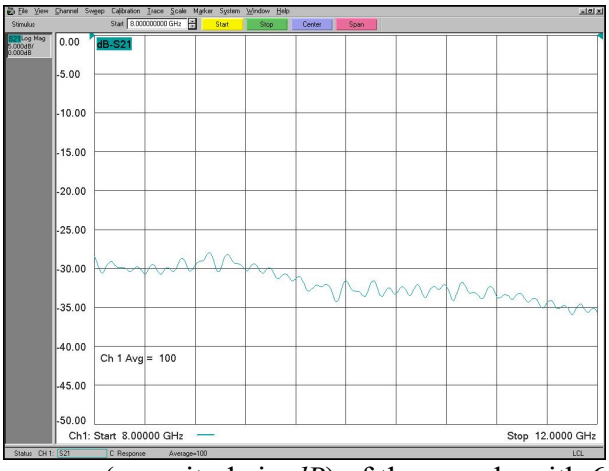

Fig. 4.7 frequency response (magnitude in *dB*) of the sample with 65% in wt of graphite

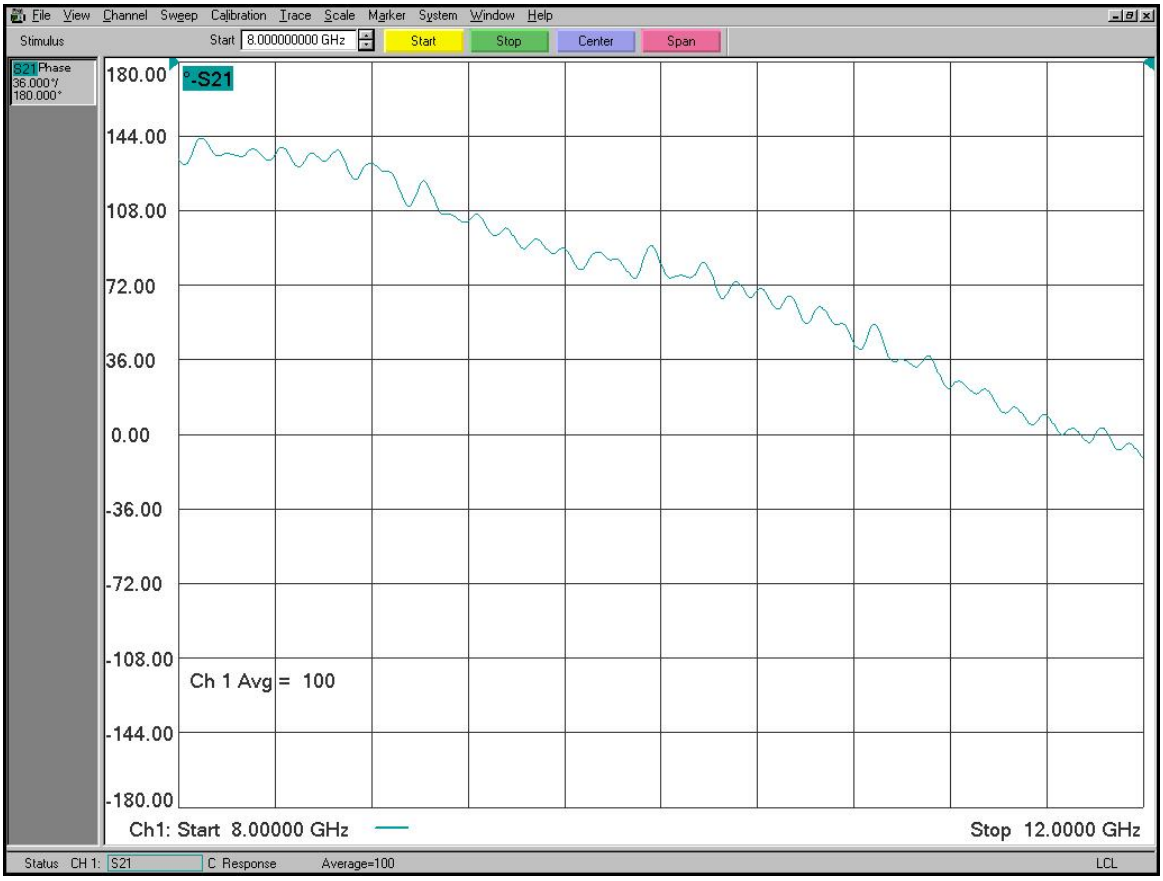

Fig. 4.8 frequency response (phase *in degrees*) of the sample with 65% in wt of graphite

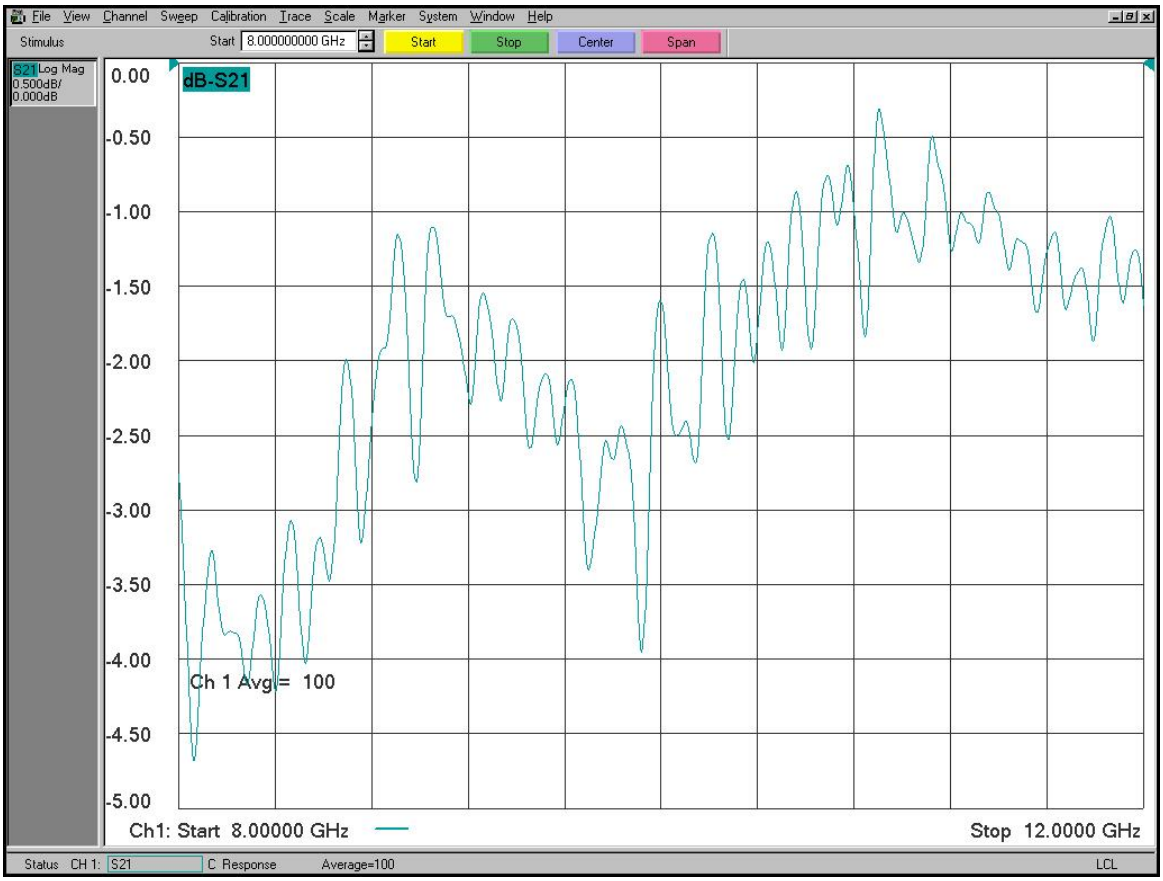

Fig. 4.9 frequency response (magnitude in *dB*) of the silicone sample

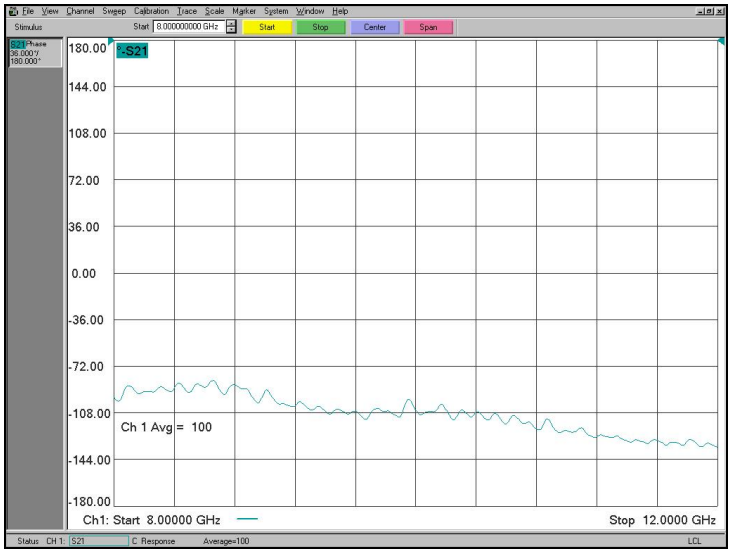

Fig. 4.10 frequency response (phase *in degrees*) of the silicone sample

After, these experimental investigations, it is necessary to analyse, for each sample typology, the selectivity behaviour. In particular, for each percentage of the particles embedded in the matrix, we have to determine the specific frequency value at which the materials provide the requested selectivity.
This is an important goal, with a broad interest in many scientific sectors and engineering applications.

5 – CONCLUSIONS

In this paper a development of innovative nanostructured FSS is illustrated. The principal activities are focalised on the technological methods necessary to manufacture these nano – materials. Particular attention is dedicated to characterizations of the base materials (polymeric matrix, curing agent, nanoparticles) using the electronic microscopy (SEM, HRTEM, and EDX). The degassing phase is essential to obtain the three following micro- and macro-properties: homogeneity, continuity and isotropic characterization. Also, the curing phase (temperature, pressure, inert conditions) characterise the final properties of the produced FSS.
The NDT testing shows that the above properties are obtained. This allows us to qualify the technological process employed.
The experimental electromagnetic test provides a interesting preliminary results. The graphics show a particular behaviour of the nanostructured FSSs. In particular, using different quantities of the nanoparticles embedded on the polymeric matrix it is possible to obtain various electromagnetic behaviours.
In particular increasing the percentage of the particles embedded in the matrix, the sample present a significant improvement of the electromagnetic absorbed by material. Besides, for each percentage it is necessary to determine the specific frequency of selectivity.
The future applications of these innovative nanomaterials are the developments of multifunctional hybrid nanostructured composite materials able to provide, simultaneously, mechanical, thermal and electromagnetic specific behaviours.

6 – ACKNOWLEDGMENTS

Special thanks to Dr. Luigi Paoletti and Dr. Biagio Bruni (ISS – Istituto Superiore di Sanità – Dipartimento di Tecnologie e Salute – Roma) for the collaboration in the nanoparticle SEM and EDX characterizations.

Thanks to Dr. Stefano Bellucci and Dr. Giorgio Giannini (Director of the Nanotecnology Laboratory and Scientific Collaborator, respectively, at INFN – Istituto Nazionale di Fisica Nucleare, Frascati – Italy) for the scientific activities in the carbon nanotubes synthesis with the CVD method.
Thanks to Dr. Giancarlo Spera (Alitalia Engineering Maintenance Division) for the NDT test of the nanostructured polymeric samples.
Thanks to Dr. Raffaele Mucciato and Dr. Gilberto Gaggiotti (2M Strumenti S.p.A.) for the collaboration in the AFM carbon nanotubes characterizations.

7 – BIBLIOGRAPHY

[1] F. Campos, A. D'Assuncao, G. Neto – SCATTERING CHARACTERISTICS OF FSS ON TWO ASINOTROPIC LAYERS FOR INCIDENT CO-POLARIZED PLANE WAVES, Microwave and Optical Technology Letters Vol. 33, n° 1, april 5 2002
[2] C. Lu, R. Chern, C. Chang – ANALYSIS OF FREQUENCY SELECTIVE SURFACES BY SPECTRAL GALERKIN METHOD, Institute of Applied Mechanics, National Taiwan University
[3] S. Cui, D. Weile – EFFICIENT ANALYSIS OF SCATTERING FOR PERIODIC STRUCTURES COMPOSED OF ARBITRARY INHOMOGENEOUS AND ANISOTROPIC MTERIALS USING FE-BI METHOD ACCELERATED BY FFT, Dept. of Electrical & Computer Engineering, University of Delaware, Newark DE
[4] J. Collins, C. Xirouchaki, J. Heat, C. Jones – CLUSTERS FOR BIOLOGY: IMMOBILIZATION OF PROTEINS BY SIZE-SELECTED METAL CLUSTERS, Applied Surface Science 226 (2004) 197-208
[5] S. Chakravarty, R. Mittra – APPLICATION OF MICRO GENETIC ALGORITHM TO THE DESIGN OF SPATIAL FILTERS WITH FREQUENCY SELECTIVE SURFACES EMBEDDED IN DIELECTRIC MEDIA, IEEE Transactions on Electromagnetic Compatibility, Vol. 44 n° 2, may 2002
[6] M. Bozzi, G. Manara, A. Monorchio, L. Perregrini – AUTOMATIC DESIGN OF INDUCTIVE FSSs USING THE GENETIC ALGORITHM AND THE MoM/BI-RME ANALYSIS, IEEE Antennas and Wireless Propagation Letters Vol. 1, 2002
[7] Y. Erdemli, K. Sertel, R. Gilbert, D. Wright, J. Volakis – FREQUENCY SELECTIVE SURFACES AND VOLUMES TO ENHANCED PERFORMANCE OF BROADBAND RECONFIGURABLE SLOT ARRAYS, T15 Antenna arrays, planar and conformal
[8] S. Chakravarty, R. Mittra – DESIGN OF A FREQUENCY SELECTIVE SURFACE (FSS) WITH VERY LOW CROSS-POLARIZATION DISCRIMINATION VIA PARALLEL MICRO GENETIC ALGORITHM, IEEE Transactions on Antennas and Propagation, Vol. 51, n° 7, july 2003
[9] S. Chakravarty, R. Mittra, N. Williams – ON THE APPLICATION OF THE MICROGENETIC ALGORITHM TO THE DESIGN OF BROAD-BAND MICROWAVE ABSORBERS COMPRISING FREQUENCY SELECTIVE SURFACES EMBEDDED IN MULTILAYERED DIELECTRIC MEDIA, IEEE Transactions on Microwave Theory and Techniques, Vol. 49, n° 6, june 2001
[10] S. Chakravarty, R. Mittra, N. Williams – APPLICATION OF MICROGENETIC ALGORITHM (MGA) TO THE DESIGN OF BRAD-BAND MICROWAVE ABSORBERS USING MULTIPLE FREQUENCY SELECTIVE SURFACE SCREENS BURIED IN DIELECTRICS, IEEE Transactions on Antennas and Propagation, Vol. 50, n° 3, march 2002
[11] H. Allouche, M. Monthioux, R. Jacobsen – CHEMICAL VAPOR DEPOSITION OF PYROLYTIC CARBON ON CARBON NANOTUBES PART 1 SYNTHESIS AND MORPHOLOGY, Carbon 41 (2003) 2897-2912

[12] C. Lee, J. Park – GROWTH AND STRUCTURE OF CARBON NANOTUBES PRODUCED BY THERMAL CHEMICAL VAPOR DEPOSITION, Carbon 39 (2001) 1891-1896
[13] Y. Shyu, F. Hong – LOW-TEMPERATURE GROWTH AND FIELD EMISSION OF ALIGNED CARBON NANOTUBES BY CHEMICAL VAPOR DEPOSITION, Materials Chemistry and Physics 72 (2001) 223-227
[14] M. Grujicic, G. Cao, B. Gersten – OPTIMIZATION OF CHEMICAL VAPOR DEPOSITION PROCESS FOR CARBON NANOTUBES FABRICATION, Applied Surface Science 191 (2002) 223-239
[15] M. Grujicic, G. Cao, B. Gersten – OPTIMIZATION OF CHEMICAL VAPOR DEPOSITION PROCESS FOR CARBON NANOTUBES FABRICATION, Applied Surface Science 199 (2002) 90-106
[16] C. Lee, S. Lyu, Y. Cho, J. Lee, K. Cho – DIAMETER-CONTROLLED GROWTH OF CARBON NANOTUBES USING THERMAL CHEMICAL VAPOR DEPOSITION, Chemical Physics Letters 341 (2001) 245-249
[17] Y. F. Zhang, Y. H. Zhang, C. Lee, I. Bello, S. Lee – DEPOSITION OF CARBON NANOTUBES ON Si NANOWIRES BY CHEMICAL VAPOR DEPOSITION, Chemical Physics Letters 330 (2000) 48-52
[18] C. Lee, J. H. Park, J. Park – SYNTHESIS OF BAMBOO SHAPED MULTIWALLED CARBON NANOTUBES USING CHEMICAL VAPOR DEPOSITION, Chemical Physics Letters 323 (2000) 560-565
[19] M. Grujicic, G. Cao, B. Gersten – AN ATOMIC SCALE ANALYSIS OF CATALYTICALLY ASSISTED CHEMICAL VAPOR DEPOSITION OF CARBON NANOTUBES, Materials Science and Engineering B94 (2002) 247-259
[20] W. Zhang, J. Thong, W. Tjiu, L. Gan – FABRICATION OF VERTICALLY ALIGNED CARBON NANOTUBES PATTERNS BY CHEMICAL VAPOR DEPOSITION FOR FILED EMITTERS, Diamond and Related Materials 11 (2002) 1638-1642
[21] M. Regi, M. Marchetti, F. Mancia, G. Allegri - SYNTHESIS OF CARBON NANOTUBES AND THEIR APPLICATION IN "ANISOGRID LATTICE STRUCTURES", Proceedings SEM X International Congress & Exposition on Experimental and Applied Mechanics, 5th International Symposium on MEMS and Nanotechnology, June 7 -10 2004 Costa Mesa California USA
[22] M. Regi, R. Mucciato, S. Bellucci, M. Marchetti, G. Gaggiotti, P. Borin, G. Giannini – STUDY AND CHARACTERIZATION OF CARBON NANOTUBES WITH THE ATOMIC FORCE MICROSCOPY (AFM), Nanoscience and Nanotechnology NN2005, INFN – LNF, Villa Mondragone Monteporzio Catone (Frascati, Roma), 14 – 16 novembre 2005
[23] S. Bellucci, C. Balasubramanian, G. Giannini, P. Borin, M. Regi, F. Micciulla – FIELD EMISSION STUDIES FROM MULTIWALLED CARBON NANOTUBES, Nanoscience and Nanotechnology NN2005, INFN – LNF, Villa Mondragone Monteporzio Catone (Frascati, Roma), 14 – 16 novembre 2005
[24] J. Romeu, Y. Samii – FRACTAL FSS: A NOVEL DUAL-BAND FREQUENCY SELECTIVE SURFACES, IEEE Transactions on Antennas and Propagation, Vol. 48, n° 7, july 2000
[25] M. S. Sarto, F. Sarto, M. C. Larciprete, M. Scalora, M. D'Amore, C. Sibilia – NANOTECHNOLOGY OF TRANSPARENT METLS FOR RADIO FREQUENCY ELECTROMAGNETIC SHIELDING, IEEE Transactions on Electromagnetic Compatibility, Vol. 45, n° 4, november 2003
[26] J. Lynch, J. Colburn – MODELLING POLARIZATION MODE COUPLING IN FREQUENCY SELECTIVE SURFACES, IEEE Transactions on Microwave Theory and Techniques, Vol. 52, n° 4, april 2004
[27] Gerhard Kristensson – HOMOGENIZATION OF SPHERICAL INCLUSIONS, Department of Electroscience Electromagnetic Theory Lund Institute of Technologies Sweden, 1 22 2002

[28] A. Karisson, D. Sjoberg, B. Widenberg – FREQUENCY SELECTIVE STRUCTURES WITH STOCHASTIC DEVIATIONS, Department of Electroscience Electromagnetic Theory Lund Institute of Technologies Sweden, 1 16 2003
[29] A. Karisson – PHYSICAL LIMITATIONS OF ANTENNAS IN A LOSSY MEDIUM, Department of Electroscience Electromagnetic Theory Lund Institute of Technologies Sweden, 1 15 2003
[30] Gerhard Kristensson – ON THE GENERATION OF SURFACE WAVES IN FREQUENCY SELECTIVE STRUCTURES, Department of Electroscience Electromagnetic Theory Lund Institute of Technologies Sweden, 2003